Development of modified HCH-1 kinetic model for long-term enzymatic cellulose hydrolysis and comparison with literature models

Chao Liang[1*], Chao Gu[2], Jonathan Raftery[1], M. Nazmul Karim[1] and Mark Holtzapple[1]

Abstract

Background: Enzymatic hydrolysis is a major step for cellulosic ethanol production. A thorough understanding of enzymatic hydrolysis is necessary to help design optimal conditions and economical systems. The original HCH-1 (Holtzapple–Caram–Humphrey–1) model is a generalized mechanistic model for enzymatic cellulose hydrolysis, but was previously applied only to the initial rates. In this study, the original HCH-1 model was modified to describe integrated enzymatic cellulose hydrolysis. The relationships between parameters in the HCH-1 model and substrate conversion were investigated. Literature models for long-term (> 48 h) enzymatic hydrolysis were summarized and compared to the modified HCH-1 model.

Results: A modified HCH-1 model was developed for long-term (> 48 h) enzymatic cellulose hydrolysis. This modified HCH-1 model includes the following additional considerations: (1) relationships between coefficients and substrate conversion, and (2) enzyme stability. Parameter estimation was performed with 10-day experimental data using α-cellulose as substrate. The developed model satisfactorily describes integrated cellulose hydrolysis data taken with various reaction conditions (initial substrate concentration, initial product concentration, enzyme loading, time). Mechanistic (and semi-mechanistic) literature models for long-term enzymatic hydrolysis were compared with the modified HCH-1 model and evaluated by the corrected version of the Akaike information criterion. Comparison results show that the modified HCH-1 model provides the best fit for enzymatic cellulose hydrolysis.

Conclusions: The HCH-1 model was modified to extend its application to integrated enzymatic hydrolysis; it performed well when predicting 10-day cellulose hydrolysis at various experimental conditions. Comparison with the literature models showed that the modified HCH-1 model provided the best fit.

Keywords: Enzymatic cellulose hydrolysis, Simulation, HCH-1, Model comparison, Sensitivity analysis

Background

Biomass is the only renewable energy resource that can be directly converted to liquid fuels and chemicals. The largest biomass feedstock is lignocellulose, which is found globally in many forms. Converting lignocellulose into biofuels could relieve shortages of liquid fuels and reduce dependence on fossil energy.

In the United States, ethanol is the dominant biofuel, which is usually produced from corn, an important food for animals and humans. To prevent food shortages, cellulosic ethanol is an attractive alternative. In general, there are four major steps for cellulosic ethanol production: pretreatment, hydrolysis, fermentation, and separation. Among these processes, hydrolysis accounts for a large portion (~ 30%) of the total costs [1]. To compete with corn ethanol and petroleum-derived gasoline, enzymatic hydrolysis needs optimization and cost reduction [2]; therefore, a thorough understanding of enzymatic

*Correspondence: liang.chao@tamu.edu
[1] Department of Chemical Engineering, Texas A&M University, College Station, TX 77843-3122, USA
Full list of author information is available at the end of the article

Liang *et al. Biotechnol Biofuels*   (2019) 12:34

Page 2 of 13

hydrolysis is necessary to help design optimal conditions and economical systems.

During the last several decades, various theoretical and empirical models have been developed to simulate enzymatic hydrolysis of cellulose [3–6]. Because they lack a theoretical foundation, empirical models cannot be applied beyond the range of the data; therefore, this paper only focuses on mechanistic (and semi-mechanistic) models.
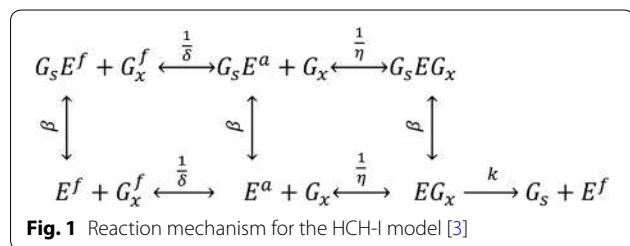
In 1984, Holtzapple et al. [3] proposed a generalized mechanistic model for cellulose hydrolysis termed the HCH-1 (Holtzapple–Caram–Humphrey-1) model. Figure 1 shows the reaction mechanism of the HCH-1 model [3]. As shown in the figure, free enzyme (E^f) adsorbs onto a free cellulose site (G_x^f) to become adsorbed enzyme (E^a), and then complexes with the cellulose to become enzyme–substrate complex (EG_x). This complex catalyzes the hydrolysis of the cellulose site to obtain soluble product (G_s) with reaction rate k. All enzyme species can complex with product to become inhibited enzyme (G_sE^f, G_sE^a, and G_sEG_x). For simplicity, the product-binding constant (β) is assumed to be the same for all the enzyme species. In addition, the adsorption constant (δ) and the complexing constant (η) are assumed not to be affected by the binding of product to the enzyme [3].

The rate-limiting step is the hydrolysis; therefore, the reaction velocity (V) is proportional to the concentration of uninhibited enzyme–substrate complex (EG_x). To express the reaction velocity in terms of known variables, substitutions can be made for EG_x using material balances of substrate and enzyme species, thus, yielding the HCH-1 model (Eq. 1). The detailed model development is described in [3].

$$V = \frac{\kappa[G_x][E]i}{\alpha + \varphi[G_x] + \varepsilon[E]}$$

$$i = \frac{1}{1 + \beta_1[G_1] + \beta_2[G_2]}$$

$$\varphi = \frac{[G_x] - \alpha - \varepsilon[E] + \sqrt{([G_x] - \alpha - \varepsilon[E])^2 + 4\alpha[G_x]}}{2[G_x]} \tag{1}$$

$$G_sE^f + G_x^f \xrightleftharpoons[]{\frac{1}{\delta}} G_sE^a + G_x \xrightleftharpoons[]{\frac{1}{\eta}} G_sEG_x$$

$$\Big\updownarrow \beta \qquad\qquad \Big\updownarrow \beta \qquad\qquad \Big\updownarrow \beta$$

$$E^f + G_x^f \xrightleftharpoons[]{\frac{1}{\delta}} E^a + G_x \xrightleftharpoons[]{\frac{1}{\eta}} EG_x \xrightarrow{k} G_s + E^f$$

Fig. 1 Reaction mechanism for the HCH-I model [3]

where G_x is the cellulose concentration (g/L, equivalent to glucose), G_1 is the glucose concentration (g/L), G_2 is the cellobiose concentration (g/L, equivalent to glucose), E is the enzyme concentration (g/L), α is the lumped adsorption constant ($\alpha = \frac{\eta\delta}{\eta+1}$, g/L), κ is the lumped kinetic constant ($\kappa = \frac{k}{\eta+1}$, h^{-1}), β_1 is the glucose binding constant (L/g), β_2 is the cellobiose binding constant (L/g), ε is the number of cellulose sites covered by adsorbed or complexed enzyme (dimensionless), i is the fraction of total enzyme that is active (dimensionless), and φ is the fraction of total cellulose sites which are free (dimensionless).

Unlike the classic Michaelis–Menten model, the HCH-1 model includes a parameter ε that describes the number of reactive sites covered by the enzymes [3, 7]. Furthermore, the HCH-1 model includes non-competitive inhibition by sugar products.

Unlike empirical models that apply only in the range where the data were taken, the HCH-1 model is mechanistic (Fig. 1) and, therefore, has broader applicability. As a mechanistic model, it applies to individual enzyme species; however, it has also been applied successfully to an enzyme cocktail in which the mixture is treated as a single "lumped" enzyme. Using the initial-rate data for pretreated biomass hydrolyzed by an enzyme cocktail, Brown et al. [7] compared mechanistic models and showed that the HCH-1 model provided the best fit to experimental data.

Previous studies show that, at high degrees of conversion, the hydrolysis rate drops by 2–3 orders of magnitude [8, 9]. The following factors contribute to the decreasing hydrolysis rates: (1) enzyme deactivation, (2) product inhibition, (3) decreased substrate reactivity, (4) decreased substrate accessibility, and (5) decreased synergism between cellulases [10]. In short-term enzymatic hydrolysis, these factors are not important and, therefore, are usually not incorporated into models that predict initial rates. However, in long-term batch saccharification, the reaction time is usually 3 to 5 days. As the reaction proceeds, the coefficients in short-term enzymatic hydrolysis models, such as HCH-1, may change because of the enumerated factors above. To describe long-term integrated enzymatic hydrolysis, the initial-rate models must be modified.

In this study, the original HCH-1 model was modified to describe 10-day enzymatic cellulose hydrolysis with commercial enzyme cocktail CTec2. The HCH-1 mechanism (Fig. 1) applies to individual enzymes in the cocktail; however, modeling each enzyme component is exceedingly complex. Understanding the kinetics of each enzyme component would be useful when optimizing the cocktail; however, this study uses a cocktail with defined components. Our approach is to treat the enzyme

cocktail as a single "lumped" enzyme; hence, the resulting "lumped" parameters reflect the collective kinetics of the cocktail, not the individual components. To describe long-term enzymatic hydrolysis, this study investigates the relationships between the "lumped" parameters in the HCH-1 model and substrate conversion. The sensitivities of parameters in the modified model were analyzed. In addition, literature models for long-term (> 48 h) enzymatic hydrolysis were summarized and compared to the modified HCH-1 model.

Materials and methods
Materials
Substrate
The substrate used for all experiments was α-cellulose (Sigma-Aldrich, C8002). Compositional analysis showed that the substrate contained glucan 78.5% and xylan 14.4% [11].

Enzyme
The enzyme used in this study was Novozymes Cellic® CTec2 (lot# VCPI 0007), a blend of aggressive cellulases with high levels of β-glucosidases and hemicellulases that degrade lignocellulose into sugars [12]. The protein concentration was determined to be 294 mg protein/mL with Pierce BCA assay [11]. Before use, the enzyme solution was diluted ten times with deionized (DI) water.

Citrate buffer
To maintain relatively high enzyme activity, citrate buffer (0.1 M) with a pH of 4.8 was used in enzymatic hydrolysis experiments. To prepare the buffer, citric acid monohydrate and trisodium citrate dihydrate were added to DI water.

Antibiotics
To prevent the growth of contaminating microorganisms that could consume produced sugars, an antibiotic cocktail was added. To prepare the solutions, tetracycline powder was dissolved in an aqueous solution of 70% ethanol at 10 g/L and cycloheximide powder was dissolved in DI water at 10 g/L.

Enzymatic hydrolysis
In the enzymatic hydrolysis experiments, desired amounts of α-cellulose, glucose, and DI water together with 125 mL citrate buffer, 2 mL tetracycline solution, and 1.5 mL cycloheximide solution were added to a 1-L centrifuge bottle in sequence and then preheated. When the mixture reached 50 °C, enzymes were added. Then, the centrifuge bottle (total working

volume of 250 mL) was placed in the incubator at 50 °C for 10 days with an axial rotation of 2 rpm. Liquid samples of 0.5 mL were taken periodically and submerged in boiling water for 20 min to deactivate the enzymes (note: the volume of liquid sample is small relative to the total slurry volume, so it is assumed to have a negligible impact on substrate concentration). Then, to determine the glucose concentration, the samples were filtered and analyzed by a high-performance liquid chromatography (HPLC), which was equipped with a pair of de-ashing guard columns (Bio-Rad Micro-Guard de-ashing cartridges, 30 mm × 4.6 mm) and an HPLC carbohydrate analysis column (Bio-Rad Aminex HPX-87P, 300 mm × 7.8 mm).

Selection of hydrolysis conditions
Experiments for model fitness
Based on our previous study [11], 16 enzymatic hydrolysis conditions were tested including four different substrate concentrations (40, 60, 80, and 100 g/L), two different enzyme loadings (2 and 5 mg protein/g of dry biomass (mg/g)), and two different initial glucose concentrations (0 and 33 g/L).

Experiments for model predictions
Three enzymatic hydrolysis conditions—which were different from the conditions used for model fitness—were tested for model predictions: (1) substrate concentration: 40 g/L, enzyme loading: 1 mg/g, initial glucose concentration: 0 g/L; (2) substrate concentration: 70 g/L, enzyme loading: 1 mg/g, initial glucose concentration: 28 g/L; (3) substrate concentration: 100 g/L, enzyme loading: 5 mg/g, initial glucose concentration: 28 g/L.

Enzyme stability
Enzyme stability was measured by quantifying the soluble protein concentration over the course of 20 days. In this experiment, the desired amount of CTec2 was added to the preheated mixture of citrate buffer, DI water, and antibiotic cocktail. The resulting solution was placed in the incubator at 50 °C. Samples of 0.5 mL were taken periodically and then centrifuged at 13,000 rpm for 10 min. The protein concentration of the supernatant was measured by the Pierce BCA method.

Modification of HCH-1 model
Simulation of enzyme stability
Wallace et al. [13] reported that unproductive binding with lignin and thermal deactivation may play a significant role in enzyme deactivation. Considering the

Liang *et al. Biotechnol Biofuels* (2019) 12:34

Page 4 of 13

substrate used in this study is lignin-free, we assume that enzyme deactivation is solely due to thermal deactivation. Rosales-Calderon et al. [14] observed that the protein concentration of a mixture of glucanase and β-glucosidase dropped 34% after incubating at 50 °C for 4 days. It was hypothesized that the enzyme proteins suffered a structural change at 50 °C, which led to protein aggregation and precipitation. Additives, whose concentration was assumed constant and proportional to the initial enzyme protein concentration, were supposed to be present in the cocktail to stabilize the enzyme protein against aggregation. Equation 2 incorporates the presence of additives and is proposed to model protein stability [14]. The development of Eq. 2 is described in detail by Rosales-Calderon et al. [14].

$$-\frac{\mathrm{d}[E]}{\mathrm{d}t} = k_1[E] - k_2([E_0] - [E])[E_0], \tag{2}$$

where E is the native enzyme protein concentration (g/L), E_0 is the initial enzyme protein concentration (g/L), and k_1 and k_2 are the rate constants (h^{-1}).

The stability of CTec2 with three different initial concentrations was tested. Equation 2 was used to fit the experimental data.

Modification of HCH-1 model

The HCH-1 model was modified by the following steps:

Step 1: Use an empirical equation (Eq. 3) to fit the experimental data of the 16 enzymatic hydrolysis conditions ("Experiments for model fitness" section) with high accuracy. This smoothed version of the data provides the reaction rates needed to fit the parameters in the modified HCH-1 model of enzymatic hydrolysis.

$$\frac{\mathrm{d}[G_1]}{\mathrm{d}t} = \frac{3.7798\left([G_x^0] - [G_1]\right)^{0.6410}\left(\frac{[E_0](0.0574[E_0] + 0.4370\exp\left(-t(0.4370 + 0.0574[E_0])\right))}{0.4370 + 0.0574[E_0]}\right)^{0.8500}}{1 + 0.0247[G_1]^{1.1579}},$$

$$\tag{3}$$

where G_x^0 is the initial cellulose concentration (g/L, equivalent to glucose).

Equation 3 was developed based on the integrated version of Eq. 2 and an empirical model for batch fermentation [15]. Detailed development of this equation is described in Additional file 1. To fit the parameters, Eq. 3 was solved with the *ode45* routine in MATLAB and nonlinear optimization was achieved by the *fmincon* routine. The objective function was the sum of square errors (SSE), which is the sum of the squared difference between

experimental data and the predicted value [16]. The optimal set of parameters corresponds to the smallest SSE value. This empirical correlation of the data provided a coefficient of determination $R^2 = 0.994$.

Step 2: Divide substrate conversion (from 0 to 1) into 50 equal segments. Using Eq. 3, calculate the reaction rate at each conversion and get a 16×50 data set.

Step 3: Determine product inhibition.

The inhibition parameter i in the HCH-1 model was calculated by determining the initial velocities with and without inhibitor (Eq. 4) [17]. To estimate this value, the same enzyme and cellulose concentrations should be used.

$$i = \frac{V_{\text{with inhibitor}}}{V_{\text{no inhibitor}}} = \frac{\left[\frac{\kappa[G_x^0][E]}{\alpha + [G_x^0] + \varepsilon[E]}\right]i}{\frac{\kappa[G_x^0][E]}{\alpha + [G_x^0] + \varepsilon[E]}} \tag{4}$$

The inhibition of enzymatic hydrolysis by cellobiose was not considered in this study, because CTec2 contains a high level of β-glucosidase that rapidly converts produced cellobiose into glucose; the cellobiose peak was not found in the HPLC results.

For a single inhibitor, the inhibition parameter i is expressed in Eq. 5 and the glucose binding constant β_1 is calculated with Eq. 6.

$$i = \frac{1}{1 + \beta_1[G_1]} \tag{5}$$

$$\beta_1 = \frac{(1 - i)}{i[G_1]} \tag{6}$$

Step 4: Use the HCH-1 model to fit the 16 reaction conditions at each conversion, and determine the best-fit coefficients κ, α, and ε.

Step 5: Determine the relationship between parameter κ and conversion x.

Figure 2a presents the relationship between parameter κ in the HCH-1 model and substrate conversion x. The data were obtained from Steps 1–4. As shown in the figure, κ drops very fast in the beginning and then stabilizes after conversion reaches 0.38. Nidetzky and Steiner [18] assumed that cellulose consists of an easily hydrolysable part and a recalcitrant part. Based on their two-substrate hypothesis, the authors derived a

Liang *et al. Biotechnol Biofuels*   (2019) 12:34

Page 5 of 13

mathematical model to describe the kinetics of cellulose hydrolysis. According to the simulation results, the obtained rate constant for easily hydrolysable cellulose was much higher than that of recalcitrant cellulose. Using α-cellulose as substrate, they determined that the fraction of easily hydrolysable cellulose was 0.3 [18]. Figure 2a can be explained by this hypothesis, but the rate constant for the easily hydrolysable cellulose decreases as conversion increases instead of being constant. In our experiments, the fraction of easily hydrolysable cellulose (0.38) is close to the result in [18].

Equation 7 was developed to describe the relationship between parameter κ and conversion x.

$$\kappa = \frac{k_3}{\left(1+x^{k_4}\right)^{k_5}} + k_6 , \qquad (7)$$

Fig. 2 a The relationship between parameter κ and conversion x. **b** The relationship between parameter ε and conversion x
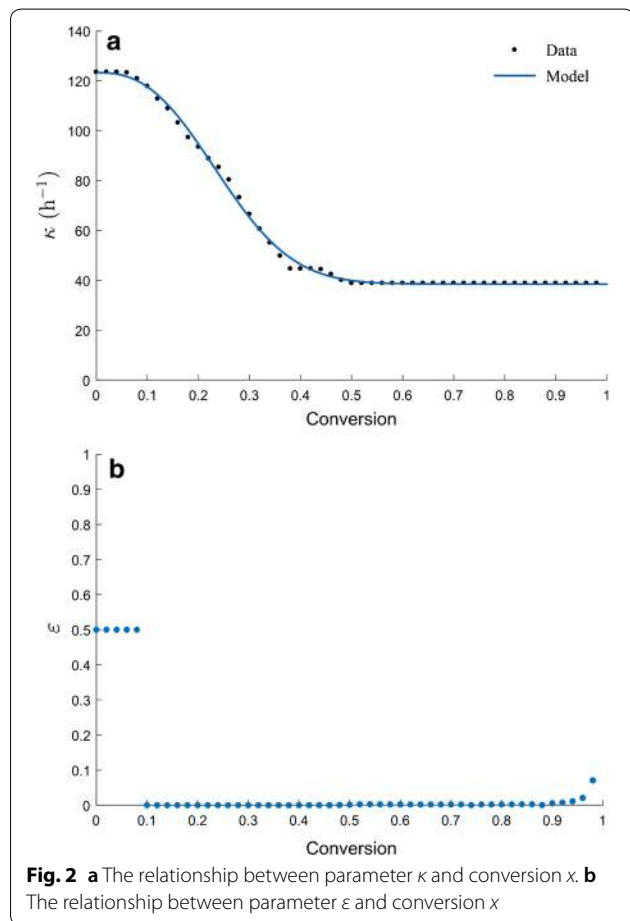
where x is the substrate conversion, k_3, k_4, k_5, and k_6 are the parameters.

The conversion x in the denominator is used to describe the negative effect of conversion on the rate constant. The parameter k_6 is considered as the rate constant for recalcitrant cellulose. The parameter k_3 is used to describe the difference in rate constants between the easily hydrolysable cellulose (initial) and recalcitrant cellulose (height of the curve). The parameters k_4 and k_5 are used to describe the decrease rate of the rate constant (steepness of the curve) for the easily hydrolysable part. To fit the data, the MATLAB curve fitting tool was used and a coefficient of determination $R^2 = 0.998$ was acquired. The values of parameters k_3, k_4, k_5, and k_6 were determined in this step.

Step 6: Determine the relationship between parameter ε and conversion x.

Figure 2b shows the relationship between parameter ε in the HCH-1 model and conversion x. As shown in the figure, parameter ε has a very narrow range (0–0.5) over the entire conversion and remains almost unchanged (nearly zero) at conversion 0.1–0.95. Therefore, in this study, parameter ε is assumed not to be affected by conversion and its optimal value should be close to zero. Brown and Holtzapple [19] reported that if $[G_x^0]/[E_0] > 35$, assuming $\varepsilon = 0$ would not introduce considerable error (< 1%) (note: in our study, $[G_x^0]/[E_0] \geq 200$). The parameter ε is needed only at high enzyme loadings. In industrial-scale saccharification, considering the high cost of enzymes, the enzyme dosage must be very low; therefore, if modeling a commercial process, the value of ε can be set as zero.

Step 7: Determine the relationship between parameter α and conversion x.

The parameter α in the original HCH-1 model may be expressed by Eq. 8, which is related to enzyme adsorption:

$$\alpha = \frac{\left[E^f\right]\left[G_x^f\right]}{[E^a]+[EG_x]} . \qquad (8)$$

Kumar and Wyman [20] showed that glucose addition and enzyme dosage can affect the percentage of cellulase adsorption. Therefore, besides the impact of conversion, the effects

Liang *et al. Biotechnol Biofuels*   (2019) 12:34

Page 6 of 13

of glucose and enzyme concentration on the value of α were tested. Using the best-fit coefficients κ and ε obtained from Step 4, two optimal α values corresponding to two initial glucose concentrations were determined by fitting the data (eight data at each initial glucose concentration) from Step 2 at each conversion with the HCH-1 model (Fig. 3a). Another two optimal α values corresponding to two enzyme concentrations were determined by repeating this procedure at each conversion (Fig. 3b). As shown in Fig. 3, as the reaction proceeds, the value of α increases and then is unchanged when the conversion reaches a certain point. It is obvious that high initial glucose concentration and low enzyme dosage improve the value of α significantly over the entire conversion range. Equation 9 was proposed to describe the relationship among α, conversion x, enzyme concentration E, and glucose concentration G_1. As shown in Fig. 3, all four curves show an "S" shape; therefore, the sigmoid function—which has an S-shaped curve—was used. The core structure of Eq. 9 is a sigmoidal function that describes the relationship between parameter α and conversion x (note: a_2 and a_3 are the parameters of the sigmoid function). In addition, because of the significant effect of glucose and enzyme concentrations on the value of α, the terms $[G_1]$ and $[E]$ were included in the numerator and denominator of the sigmoid function, respectively. The parameter a_1 was added to describe the weight of terms $[G_1]$ and $[E]$.

$$\alpha = \frac{a_1[G_1]}{[E](1+\exp(-a_2x+a_3))}, \tag{9}$$

where a_1, a_2, and a_3 are the parameters.

Step 8:   Modify HCH-1 model.

Summarizing the proposed equations, Eq. 10 is the modified HCH-1 model, where k_1, k_2, k_3, k_4, k_5, k_6, a_1, a_2, a_3, ε, and β_1 are parameters. Estimates for k_1, k_2, k_3, k_4, k_5, k_6, and β_1 were determined in previous steps. In this step, the optimal values of a_1, a_2, a_3, and ε were determined by simultaneously fitting the experimental data of the 16 enzymatic hydrolysis conditions (Section: Experiments for model fitness) with Eq. 10.
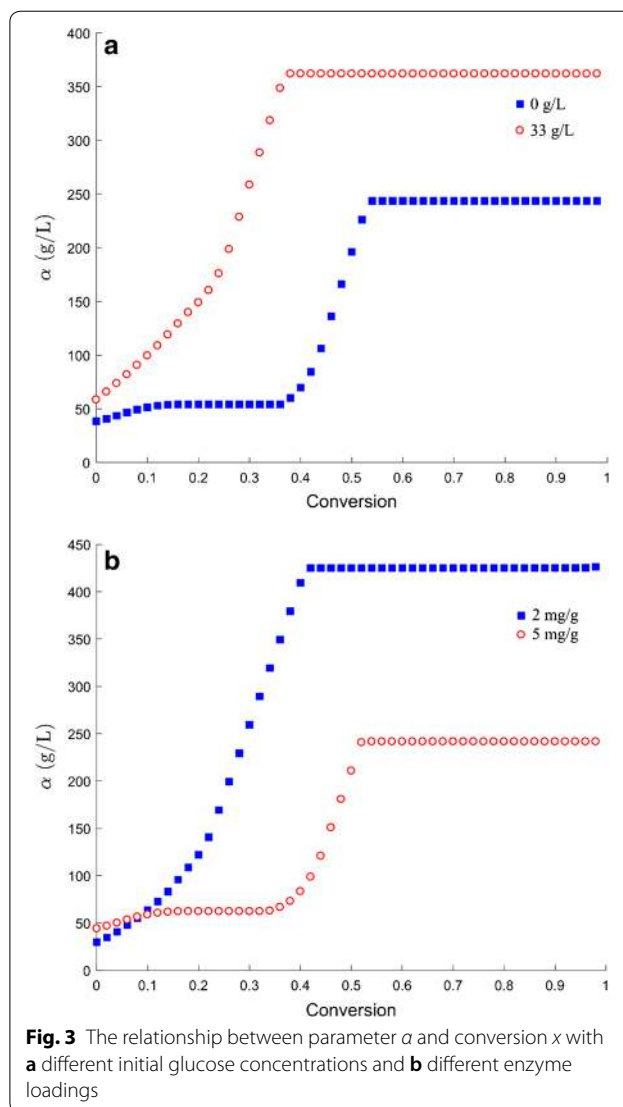
Fig. 3 The relationship between parameter a and conversion x with **a** different initial glucose concentrations and **b** different enzyme loadings

$$\frac{d[G_1]}{dt} = \frac{\kappa[G_x][E]i}{\alpha + \varphi[G_x] + \varepsilon[E]},$$

where,

$$i = \frac{1}{1 + \beta_1[G_1]}$$

$$\varphi = \frac{[G_x]-\alpha-\varepsilon[E]+\sqrt{([G_x]-\alpha-\varepsilon[E])^2+4\alpha[G_x]}}{2[G_x]}$$

$$-\frac{d[E]}{dt} = k_1[E] - k_2([E_0] - [E])[E_0]$$

$$\kappa = \frac{k_3}{\left(1 + x^{k_4}\right)^{k_5}} + k_6$$

Liang *et al. Biotechnol Biofuels*   (2019) 12:34

Page 7 of 13

$$\alpha = \frac{a_1[G_1]}{[E](1+\exp(-a_2x+a_3))} . \tag{10}$$

Integration of the differential equations described in Eq. 10 was performed using the same numerical methods described in Step 1.

Sensitivity analysis

Local sensitivity analysis

Local sensitivity analysis assesses the local impact of variation in input factors on model outputs. To do this analysis, the direct differential method [21] was used by calculating the sensitivity indices (Eq. 11). The sensitivities of parameters k_1, k_2, and β_1 were not analyzed, because their values were obtained from independent experiment or calculation.

$$S_{p_j} = \frac{\partial y}{\partial p_j} \frac{p_j}{y} , \tag{11}$$

where S_{p_j} is the non-dimensional sensitivity index of the *j*th parameter, y is the glucose concentration (g/L), and p_j is the *j*th parameter in the parameter vector p.

Global sensitivity analysis

Local sensitivity only analyzes the sensitivity of a solution close to the optimal parameter set. In contrast, global sensitivity analysis assesses the sensitivity of the model for the full range of possible parameter values [16]. In addition, global sensitivity indices can evaluate the combined impact of multiple parameters on model output.

To calculate a global sensitivity index, a normally distributed search of parameter space using the Monte Carlo method was performed and subsequent analysis of the variance in the model outputs was used. In this study, two global sensitivity indices were calculated: first-order index and total-effect index [16, 22]. The first-order index measures the effect of the parameter of interest alone on the output variance. The total-effect index accounts for not only the effect of the parameter of interest, but also interactions between the other parameters and the parameter of interest at any order.

Model evaluation

The modified HCH-1 model was compared with the literature models for long-term enzymatic hydrolysis. As described in Step 1, the same differential equation integration method, nonlinear optimization constraint algorithm, and objective function were used. The Akaike information criterion (AIC) was used to evaluate model quality for the experimental data. The corrected version of AIC (Eq. 12) was used, because the number of observations was not large enough:

$$\mathrm{AIC}_C = N \cdot \ln\left(\frac{\mathrm{SSE}}{N}\right) + 2(P+1) + 2\frac{(P+1)(P+2)}{N-P} , \tag{12}$$

where N is the number of observations, P is the number of model parameters, and SSE is the sum square error.

Results and discussion

Enzyme deactivation

Figure 4 shows that, after incubating at 50 °C for 20 days, soluble protein concentrations of CTec2 dropped to 74, 77, and 83% of their initial values of 0.15, 0.26, and 0.61 g/L, respectively. This result is consistent with a previous study [14] that shows higher initial protein concentrations favor lower deactivation rates and supports the additive hypothesis. Equation 2 successfully describes the time profiles of CTec2 protein concentration with a coefficient of determination $R^2 = 0.999$. The rate constants in Eq. 2 were determined to be $k_1 = 0.0225$ h^{-1} and $k_2 = 0.1740$ L/(g h). It should be noted that the modified HCH-1 model is a "lumped" model, the performance of each enzyme was not modeled individually; therefore, the stability of each component in the enzyme cocktail was not investigated. Equation 2 describes the overall deactivation of the cocktail.

Production inhibition

Table 1 lists the values of glucose-binding constant calculated from various reaction conditions. The eight β_1 values are very close to each other and have a standard deviation of 6×10^{-6} L/g. The mean value 0.0429 L/g is considered to be the "true" β_1 value and is used for later calculations.
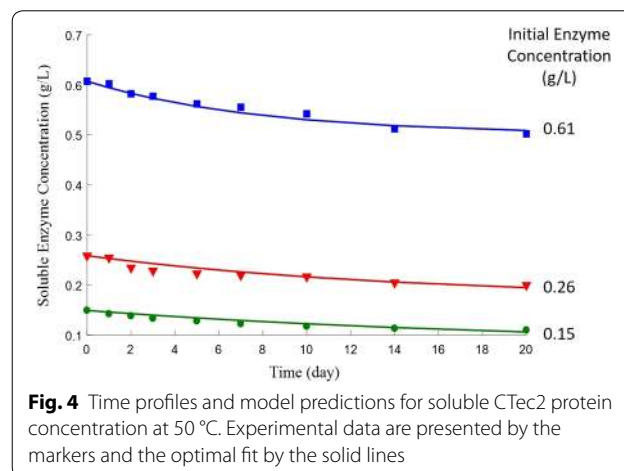
Fig. 4 Time profiles and model predictions for soluble CTec2 protein concentration at 50 °C. Experimental data are presented by the markers and the optimal fit by the solid lines

Model validation

Figure 5a shows the experimental data and modified HCH-1 model fitting results for enzymatic hydrolysis with 16 reaction conditions ("Experiments for model fitness" section). Table 2 shows the values of the parameters obtained from the previous section. The model simulation provided the coefficient of determination $R^2 = 0.992$, which indicates that the modified HCH-1 model describes enzymatic hydrolysis of α-cellulose very well.

As a comparison, Fig. 5b shows the original HCH-1 model fit to the experimental data with 16 reaction conditions ("Experiments for model fitness" section). The value of β_1 (0.0429 L/g) was obtained from the previous section (product inhibition). The optimal values ($\alpha = 2.0776 \times 10^6$ g/L, $\kappa = 9.2889 \times 10^5$ h^{-1}, and $\varepsilon = 0.9996$) were determined (note: because the original HCH-1 model was not developed for integrated cellulose hydrolysis, these parameter values are not be meaningful). The model simulation provided the coefficient of determination $R^2 = 0.947$. The calculated SSE and AICc are listed in Table 3.

Model predictions

The modified HCH-1 model (Eq. 10) was used to predict the experimental results of the three conditions described in "Experiments for model prediction." The parameter values were obtained from the fitness of the 16 conditions (Table 2). The experimental and predicted results are shown in Fig. 5c. The simulation provided the coefficient of determination $R^2 = 0.991$, which indicates that the modified HCH-1 model predicts enzymatic hydrolysis of α-cellulose with high accuracy.

Sensitivity analysis

To explore the controlling factors in the proposed model at different hydrolysis stages, local and global sensitivity analyses were performed. Figure 6a shows the parameter sensitivity indices from local sensitivity analysis of the modified HCH-1 model over the course of 10 days. As shown in the figure, the sensitivity of k_3 drops to nearly 10% of its initial value at day 10. The sensitivity of k_4 increases first and reaches up to 0.4 at around day 1, and then slightly decreases from day 2 to day 10. For the parameters about α, the sensitivity of a_1 (absolute value) increases as the hydrolysis time increases. The sensitivities of a_2 and a_3 only change within the first several reaction days, and then are close to zero after day 3. The sensitivity of ε is close to zero during the entire reaction time.

Figure 6b, c shows the global sensitivity analysis results of the modified HCH-1 model. According to the figures, the first-order indices and total-effect indices of all variables are almost identical at any time, which means that the variance in this model is not related to any interaction between parameters. At the initial stage of hydrolysis, the variance in the model output only depends on k_3 and k_6. Then, the sensitivity index of k_3 decreases very fast during the first 2 days, whereas k_4 increases up to 0.6. From day 2 to day 10, the effects of k_6 and a_1 on the model increase. The variables a_2, a_3, and ε do not show significant effects on the variance in model predictions.

According to Fig. 6, the local and global sensitivity analyses of the modified HCH-1 model show a similar trend during the entire reaction time. Figure 7 shows the sensitivity indices calculated from both analyses at day 10. The rankings of the eight sensitivity indices from both analyses are almost the same ($k_6 > a_1 > k_4 > k_5 > k_3 > a_2 \approx a_3 \approx \varepsilon$).

The sensitivity analyses not only determine which parameters have the most influence on model results, but also verify the assumption in Step 6 that the parameter ε is not needed at low enzyme loadings. These analyses provide direction for further modification of the HCH-1 model to apply it to real-world lignocellulose that contains lignin.

Model comparison

Based on the methodology used, the published mechanistic and semi-mechanistic models for cellulose and lignocellulose can be broadly divided into two classes: Michaelis–Menten and enzyme-adsorption models [10]. The models following Michaelis–Menten kinetics can also be divided into two subclasses: full Michaelis–Menten models (all rate equations follow Michaelis–Menten kinetics, including the steps of cellulose to cellobiose, cellulose to glucose, and cellobiose to glucose) and partial Michaelis–Menten models (only the step of cellobiose to glucose follows these kinetics). Models

Table 1 Glucose-binding constant from various reaction conditions

Reaction condition		β_1 (L/g)
Substrate concentration (g/L)	Enzyme loading (mg/g)	
40	2	0.042908
40	5	0.042915
60	2	0.042912
60	5	0.042918
80	2	0.042920
80	5	0.042923
100	2	0.042922
100	5	0.042925
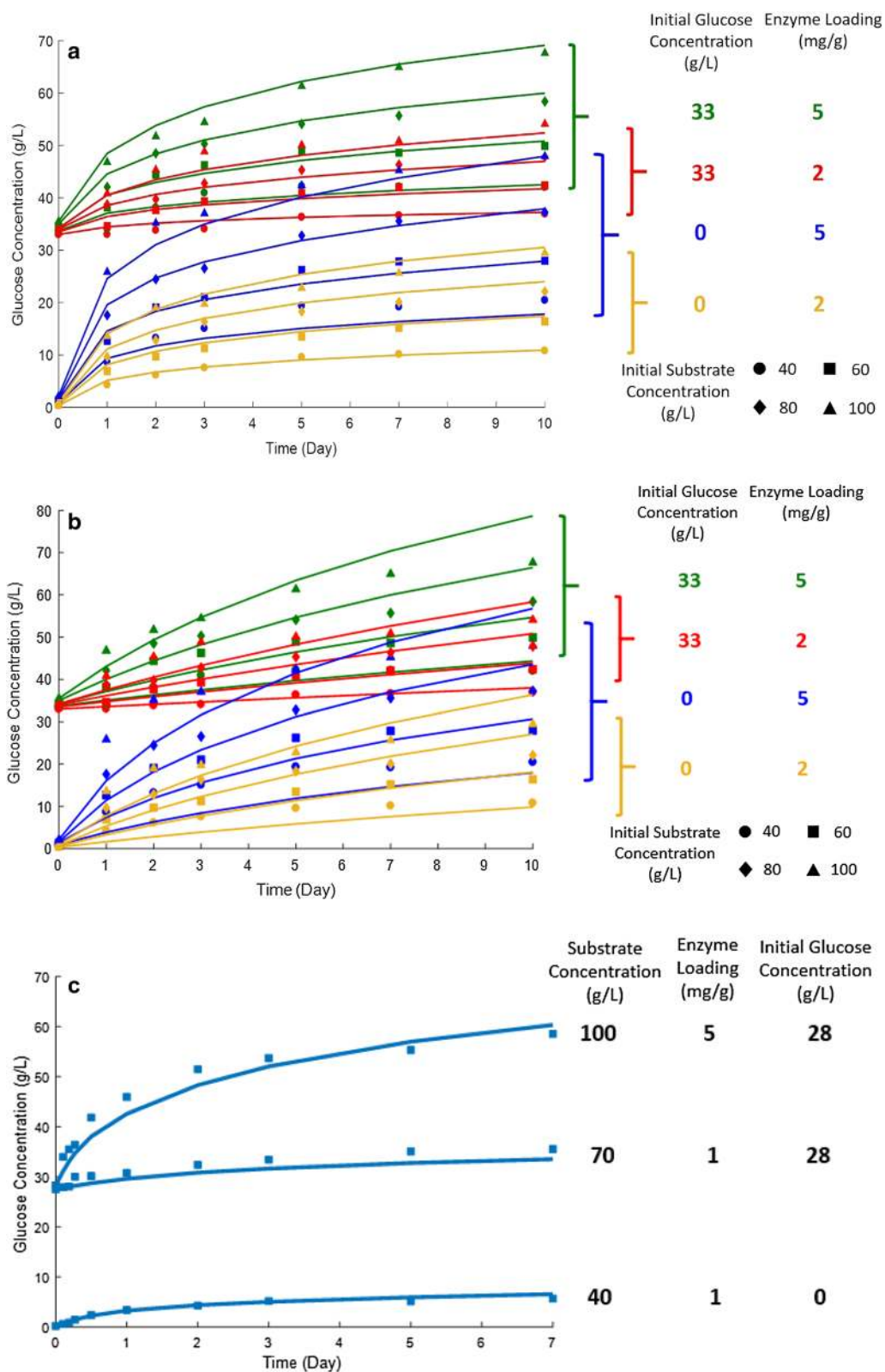
Fig. 5 a Time profiles and modified HCH-1 model fitting results for enzymatic hydrolysis of α-cellulose. **b** Time profiles and original HCH-1 model fitting results for enzymatic hydrolysis of α-cellulose. **c** Time profiles and modified HCH-1 model predictions for enzymatic hydrolysis of α-cellulose. Experimental data are presented by the markers and the values of parameters are from Table 2

Liang *et al. Biotechnol Biofuels* (2019) 12:34

Page 10 of 13

Table 2 Optimal parameter estimates for the modified HCH-1 model

Parameter	Value	Unit
k_1	0.0225	h^{-1}
k_2	0.1740	L/(g h)
k_3	84.7500	h^{-1}
k_4	2.5800	Dimensionless
k_5	26.3600	Dimensionless
k_6	38.5000	h^{-1}
a_1	1.6791	g/L
a_2	31.1485	Dimensionless
a_3	2.8452	Dimensionless
ε	5.5248×10^{-5}	Dimensionless
β_1	0.0429	L/g

employing enzyme adsorption typically use Langmuir adsorption isotherms or the help of kinetic equations [10]. Some literature models incorporate both enzyme adsorption and Michaelis–Menten kinetics.

In this study, the published models for long-term enzymatic hydrolysis of cellulose and lignocellulose were fit to the experimental data using the numerical methods described in Step 1. Some models do not consider product inhibition. To make a fair comparison, these models were only fit to experimental conditions with no initial sugar added (0 g/L initial glucose; four substrate concentrations × two enzyme loadings). Some models teased out fine details in the elementary reaction steps and

included some variables that were not determined in this study, such as exocellulase concentration and associated enzyme concentration [23–25]. These models are not included in this section. Table 3 summarizes the number of observations and parameters, calculated SSE and AICc values, and the methodology used for the published models. According to the table, the modified HCH-1 model has the least SSE and AICc values, which indicates that this model provides the best fit for long-term enzymatic hydrolysis of α-cellulose.

Conclusion

The original HCH-1 model was modified to extend its application to integrated enzymatic hydrolysis; it performed well when fitting 10-day cellulose hydrolysis at various experimental conditions. Local and global sensitivity analyses were performed to determine the controlling parameters at different hydrolysis stages. Mechanistic (and semi-mechanistic) literature models for long-term enzymatic hydrolysis were compared with the modified HCH-1 model and evaluated by AICc. Comparison results show that the modified HCH-1 model provides the best description of enzymatic cellulose hydrolysis. The "lumped" modified HCH-1 model developed in this study has a simpler form and fewer parameters than mechanistic models of each enzyme component. When each enzyme is modeled separately, the kinetics is extremely complex with the potential to over-parameterize. For the specific commercial enzyme cocktail used in this study, excellent fits to the data were

**Table 3 Comparison of long-term enzymatic hydrolysis models**

Model	N (Obs)	Parameter	SSE	AICc	Methodology
Modified HCH-1 (16)	112	11	236.7	110.9	Ads
Holtzapple et al. [3] (original HCH-1)	112	4	1630.7	310.5	Ads
Drissen et al. [26]	112	11	600.8	215.2	Ads, M–M
Fan and Lee [27]	112	11	679.7	229.0	Ads
Liao et al. [28]	112	5	1313.7	288.5	Ads
Peri et al. [21]	112	12	2657.6	384.3	Ads, M–M
Fenila and Shastri [5]	112	22	2080.9	385.5	Ads, M–M
Kadam et al. [4]	112	18	2338.6	386.4	Ads, M–M
Gusakov et al. [29]	112	16	2879.2	404.0	M–M
Philippidis et al. [30]	112	7	9139.8	510.4	Ads, M–M
Modified HCH-1 (8)[a]	56	11	115.2	71.3	Ads
Shen and Agblevor [31][a]	56	4	493.8	133.1	Ads
Zhang et al. [32][a]	56	3	692.6	149.6	Ads
Rosales-Calderon et al. [33][a]	56	3	692.6	149.6	Ads
Nidetzky and Steiner [18][a]	56	5	743.9	158.5	Ads

M–M Michaelis–Menten kinetics, *Ads* adsorption-based approach

[a] Only eight reaction conditions were fit [0 g/L initial glucose, four substrate concentrations (40, 60, 80, and 100 g/L) × two enzyme loadings (2 and 5 mg/g)]
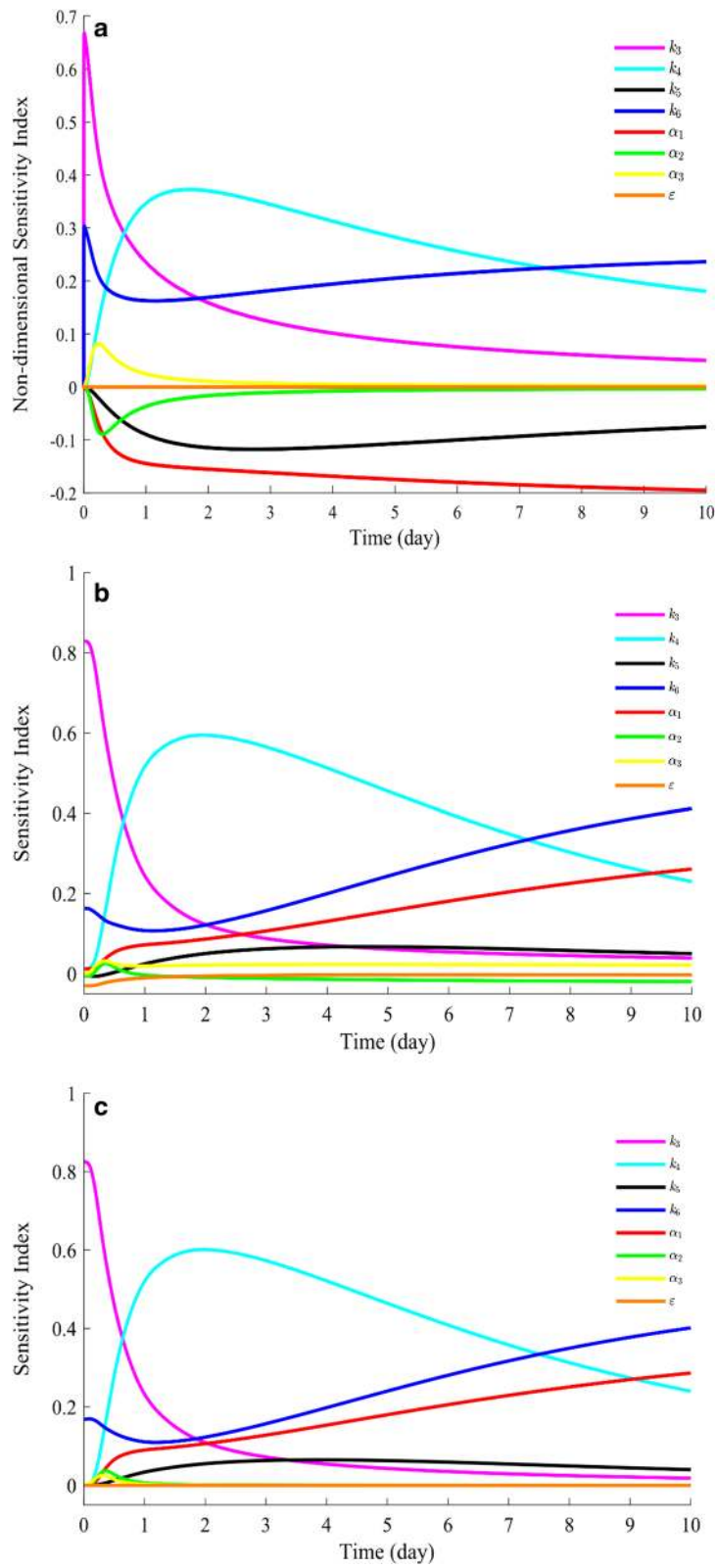
Fig. 6 **a** Local sensitivity analysis of the modified HCH-1 model at the optimal solution. Global sensitivity analysis of the modified HCH-1 model over the course of 10 days, **b** first-order indices; **c** total-effect indices

Fig. 7 The local and global sensitivity indices of the modified HCH-1 model at day 10. **a** Local sensitivity analysis and **b** global sensitivity analysis (first-order indices)
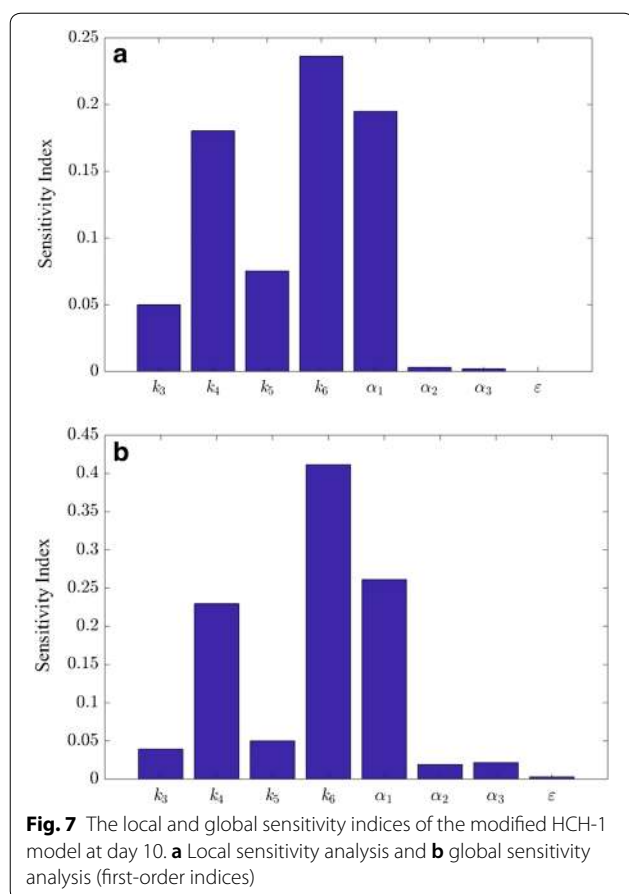
obtained without the need to model each enzyme component individually.

Additional file

Additional file 1. Development of Eq. 3.

Abbreviations
mg/g: mg protein/g of dry biomass; AIC: Akaike information criterion; SSE: sum of square errors; DI water: deionized water; M–M: Michaelis–Menten kinetics; Ads: adsorption-based approach.

Authors' contributions
CL, MNK, and MH conceived the study and participated in its design. CL performed all the experiments and drafted the manuscript. All authors were involved in the development of the model, sensitivity analysis, and model evaluation. CL, MNK, and MH revised the manuscript. All authors read and approved the final manuscript.

Author details
[1] Department of Chemical Engineering, Texas A&M University, College Station, TX 77843-3122, USA. [2] Department of Educational Psychology, Texas A&M University, College Station, TX 77843-3122, USA.

References
1. Wallace R, Ibsen K, McAloon A, Yee W. Feasibility study for co-locating and integrating ethanol production plants from corn starch and lignocellulosic feedstocks (revised). Golden: National Renewable Energy Lab; 2005.
2. Wooley R, Ruth M, Glassner D, Sheehan J. Process design and costing of bioethanol technology: a tool for determining the status and direction of research and development. Biotechnol Prog. 1999;15:794–803.
3. Holtzapple MT, Caram HS, Humphrey AE. The HCH-1 model of enzymatic cellulose hydrolysis. Biotechnol Bioeng. 1984;26:775–80.
4. Kadam KL, Rydholm EC, McMillan JD. Development and validation of a kinetic model for enzymatic saccharification of lignocellulosic biomass. Biotechnol Prog. 2004;20:698–705.
5. Fenila F, Shastri Y. Optimal control of enzymatic hydrolysis of lignocellulosic biomass. Resour Effic Technol. 2016;2:S96–104.
6. Zhou J, Wang YH, Chu J, Luo LZ, Zhuang YP, Zhang SL. Optimization of cellulase mixture for efficient hydrolysis of steam-exploded corn stover by statistically designed experiments. Bioresour Technol. 2009;100:819–25.
7. Brown RF, Agbogbo FK, Holtzapple MT. Comparison of mechanistic models in the initial rate enzymatic hydrolysis of AFEX-treated wheat straw. Biotechnol Biofuels. 2010;3:6.
8. Bommarius AS, Katona A, Cheben SE, Patel AS, Ragauskas AJ, Knudson K, Pu Y. Cellulase kinetics as a function of cellulose pretreatment. Metab Eng. 2008;10:370–81.
9. Hong J, Ye X, Zhang YH. Quantitative determination of cellulose accessibility to cellulase based on adsorption of a nonhydrolytic fusion protein containing CBM and GFP with its applications. Langmuir. 2007;23:12535–40.
10. Bansal P, Hall M, Realff MJ, Lee JH, Bommarius AS. Modeling cellulase kinetics on lignocellulosic substrates. Biotechnol Adv. 2009;27:833–48.
11. Zentay AN, Liang C, Lonkar S, Holtzapple MT. Countercurrent enzymatic saccharification of cellulosic biomass. Biomass Bioenergy. 2016;90:122–30.
12. Novozymes: cellulosic ethanol—novozymes Cellic® CTec2 and HTec2—enzymes for hydrolysis of lignocellulosic. 2010. http://www.shinshu-u.ac.jp/faculty/engineering/chair/chem010/manual/Ctec2.pdf. Accessed 29 Sep 2018.

Liang *et al. Biotechnol Biofuels*   (2019) 12:34

Page 13 of 13

13. Wallace J, Brienzo M, García-Aparicio MP, Görgens JF. Lignin enrichment and enzyme deactivation as the root cause of enzymatic hydrolysis slowdown of steam pretreated sugarcane bagasse. New Biotechnol. 2016;33:361–71.

14. Rosales-Calderon O, Trajano HL, Duff SJ. Stability of commercial glucanase and β-glucosidase preparations under hydrolysis conditions. PeerJ. 2014;2:e402.

15. Fu Z, Holtzapple MT. Anaerobic mixed-culture fermentation of aqueous ammonia-treated sugarcane bagasse in consolidated bioprocessing. Biotechnol Bioeng. 2010;106:216–27.

16. Ordoñez MC, Raftery JP, Jaladi T, Chen X, Kao K, Karim MN. Modelling of batch kinetics of aerobic carotenoid production using *Saccharomyces cerevisiae*. Biochem Eng J. 2016;114:226–36.

17. Holtzapple M, Cognata M, Shu Y, Hendrickson C. Inhibition of *Trichoderma reesei* cellulase by sugars and solvents. Biotechnol Bioeng. 1990;36:275–87.

18. Nidetzky B, Steiner W. A new approach for modeling cellulase–cellulose adsorption and the kinetics of the enzymatic hydrolysis of microcrystalline cellulose. Biotechnol Bioeng. 1993;42:469–79.

19. Brown RF, Holtzapple MT. Parametric analysis of the errors associated with the Michaelis–Menten equation. Biotechnol Bioeng. 1990;36:1141–50.

20. Kumar R, Wyman CE. An improved method to directly estimate cellulase adsorption on biomass solids. Enzyme Microb Technol. 2008;42:426–33.

21. Peri S, Karra S, Lee YY, Karim MN. Modeling intrinsic kinetics of enzymatic cellulose hydrolysis. Biotechnol Prog. 2007;23:626–37.

22. Sobol IM. Global sensitivity indices for nonlinear mathematical models and their Monte Carlo estimates. Math Comput Simul. 2001;55:271–80.

23. Shang BZ, Chang R, Chu JW. Systems-level modeling with molecular resolution elucidates the rate-limiting mechanisms of cellulose decomposition by cellobiohydrolases. J Biol Chem. 2013;288:29081–9.

24. Cruys-Bagger N, Alasepp K, Andersen M, Ottesen J, Borch K, Westh P. Rate of threading a cellulose chain into the binding tunnel of a cellulase. J Phys Chem B. 2016;120(25):5591–600.

25. Jeoh T, Cardona MJ, Karuna N, Mudinoor AR, Nill J. Mechanistic kinetic models of enzymatic cellulose hydrolysis—a review. Biotechnol Bioeng. 2017;114:1369–85.

26. Drissen RE, Maas RH, Van Der Maarel MJ, Kabel MA, Schols HA, Tramper J, Beeftink HH. A generic model for glucose production from various cellulose sources by a commercial cellulase complex. Biocatal Biotransformation. 2007;25:419–29.

27. Fan LT, Lee YH. Kinetic studies of enzymatic hydrolysis of insoluble cellulose: derivation of a mechanistic kinetic model. Biotechnol Bioeng. 1983;25:2707–33.

28. Liao W, Liu Y, Wen Z, Frear C, Chen S. Kinetic modeling of enzymatic hydrolysis of cellulose in differently pretreated fibers from dairy manure. Biotechnol Bioeng. 2008;101:441–51.

29. Gusakov AV, Sinitsyn AP, Klyosov AA. Kinetics of the enzymatic hydrolysis of cellulose: 1. A mathematical model for a batch reactor process. Enzyme Microb Technol. 1985;7:346–52.

30. Philippidis GP, Smith TK, Wyman CE. Study of the enzymatic hydrolysis of cellulose for production of fuel ethanol by the simultaneous saccharification and fermentation process. Biotechnol Bioeng. 1993;41:846–53.

31. Shen J, Agblevor FA. Kinetics of enzymatic hydrolysis of steam-exploded cotton gin waste. Chem Eng Commun. 2008;195:1107–21.

32. Zhang Y, Xu JL, Xu HJ, Yuan ZH, Guo Y. Cellulase deactivation based kinetic modeling of enzymatic hydrolysis of steam-exploded wheat straw. Bioresour Technol. 2010;101:8261–6.

33. Rosales-Calderon O, Trajano HL, Posarac D, Duff SJ. Modeling of oxygen delignified wheat straw enzymatic hydrolysis as a function of hydrolysis time, enzyme concentration, and lignin content. Ind Biotechnol. 2016;12:176–86.